Unexpected Bipolar Flagellar Arrangements and Long-Range Flows Driven by Bacteria near Solid Boundaries

Luis H. Cisneros and John O. Kessler
*Department of Physics, University of Arizona, 1118 E 4th St, Tucson, Arizona 85721, USA**

Ricardo Ortiz and Ricardo Cortez
Department of Mathematics, Tulane University, 6823 St. Charles Avenue, New Orleans, Louisiana 70118, USA+

Martin A. Bees
Department of Mathematics, University of Glasgow, Glasgow, G12 8QW, United Kingdom‡
(Received 16 May 2008; published 16 October 2008)

Experiments and mathematical modeling show that complex flows driven by unexpected flagellar arrangements are induced when peritrichously flagellated bacteria are confined in a thin layer of fluid, between asymmetric boundaries. The flagella apparently form a dynamic bipolar assembly rather than the single bundle characteristic of free swimming bacteria, and the resulting flow is observed to circulate around the cell body. It ranges over several cell diameters, in contrast to the small extent of the flows surrounding free swimmers. Results also suggest that flagellar bundles on bacteria that lie flat on a solid substrate have an effective rotation rate slower than ''free'' flagella. This discovery extends our knowledge of the dynamic geometry of bacteria and their flagella, and reveals new mechanisms for motility-associated molecular transport and intercellular communication.

DOI: 10.1103/PhysRevLett.101.168102 PACS numbers: 47.63.Gd, 47.63.mf, 87.18.Fx, 87.18.Gh

Introduction.—The geometry and dynamics of flow around active bacteria [1] determine cell-cell interactions, chemical communication, and transport. When cells are adjacent to surfaces, these flows are especially significant for the distribution of exuded polymers involved in the synthesis of biofilms [2]. *Bacillus subtilis* are rod-shaped bacteria, typically 4 μm long with a diameter of 1 μm, propelled by 6 or more helical flagella [3] randomly (i.e., peritrichously) distributed about cell body. The flagella are stiff helical polymeric structures (6–20 μm long; 20 nm diameter; 3 μm pitch; rotating at $\sim$100 Hz) attached by flexible joints to motors embedded in the cell wall [1,4]. Flagella on swimming bacteria conventionally are thought to adopt one of two arrangements. Mutual hydrodynamic attraction between flagella produces a single, polar, and corotating bundle posterior to a (requisitely) swimming cell. Reverse rotation of one or more motors produces unbundling, yielding incoherent flagellar deployment and cell tumbling (random reorientation) [4–7].

We report novel flagella-driven flows that circulate about cells of *B. subtilis* immobilized at a solid surface. These flows imply that the surface induces an unexpected geometry: a bipolar arrangement of flagellar bundles. The flows, the associated spatial arrangement of flagella, and supporting evidence from a mathematical model constitute a sea change in the understanding of the physics of fluid motion due to bacteria in the vicinity of solid boundaries. When several bacteria are arranged in close proximity, as in natural situations, we find that they drive cell-scale unsteady circulation that facilitates long-range transport and mixing [8–10]. Recent and consistent results [10] describe mixing close to a boundary enhanced by the attachment of a dense carpet of bacteria (flow due to individuals, however, was not reported).

Materials and methods.—B. subtilis 1085B was cultured in Ezmix Terrific Broth (TB; Sigma: 47.6 g broth mix and 8 mL glycerin /L distilled water). Samples were prepared by adding 1 mL stock (−20 °C) to 50 mL TB (18 h shaker-bath incubation; 37 °C; 100 rpm). Plates of 50 mL of TB were inoculated with 1 mL of suspension, and 5 h incubation obtains long, motile cells. Then, 1:100 dilutions were prepared with fresh TB and carboxylate-modified microspheres (Molec. Probes: F8809 - FluoSpheres 0.21 μm), as passive tracers.

A drop of this bacteria-bead suspension was placed on a glass coverslip, then partially removed with a pipette, yielding a thin layer of fluid. Cells were trapped between glass and meniscus at depths of $\approx$1 μm at the drop edge.

Imaging used an inverted microscope (Nikon Diaphot 300; 100x objective) with a high-speed camera (Phantom V5; 100 Hz at 256 × 256 pixel resolution). Samples were enclosed within a chamber containing water reservoirs to control humidity and avoid evaporative flows. Particle-image-velocimetry software (Dantec) was used to estimate velocity fields from image sequences.

Experimental results.—By observing the motion of passive tracers, we can estimate the flagella-driven flow. We analyze two cases: when cells are stuck between the upper ''free'' and lower ''no-slip'' boundaries, and when they are a body length from the boundaries and so free to swim with standard kinetics, but are still confined to the shallow fluid layer.

(i) Stuck cells.—Swimming bacteria may become trapped near the edge of the drop where the fluid is shallow. This is most likely due to wedging of the cell between solid and free surfaces (interfacial forces) or electrostatic attraction. In Fig. 1, we present the flow field around one such immobile bacterium. Although this organism appears ready to divide, the result is typical of stuck cells.

Figure 1 shows two-dimensional streamlines (lines such that $dx/u_x = dy/u_y$, where u_x and u_y are flow velocity components). The lengths of the arrows indicate that the flow decays rapidly with distance from the cell body.

The most startling geometric feature of the flow is its circulation. The geometry of this flow is unexpected, and it does not fit the standard models of bacteria as bodies with single polar flagellar bundles [5–7]. (Inactive cells, either dead or deflagellated, do not generate flow.) We explore this observation by sampling the velocity field along the principal axes: set **U** and **V** equal to the velocity measured along and perpendicular to the cell axis, respectively. The magnitudes of these quantities provide a measure of how the flow decays with distance (Fig. 2). Furthermore, it is clear that the flow rotates around the cell body, but also that there is flow "outwards" along the parallel axis and "inwards" along the perpendicular axis, suggesting stresslet-like flow added to the circulation and hinting at the presence of flagellar bundles with similar orientation to the cell body. Equivalent results were obtained for other stuck bacteria (we observed 25 such flows out of 27 observations of stuck cells of various lengths, i.e., in various stages of growth). The magnitude of the flow is best fitted by an exponential in the region close to the cell (within 2 body lengths), before velocities become commensurate with noise. As a function of D, distance from the center of the cell, $\mathbf{V} \propto e^{-kD}$ where $k \approx \frac{1}{4}\ \mu\mathrm{m}^{-1}$ [when average behavior along all directions is measured, $k = (0.26 \pm 0.033)\ \mu\mathrm{m}^{-1}$]. Any far-field polynomial dependence is experimentally occluded by noise, but the exponential near-field behavior can be interpreted as arising from the sum of many distributed singular solutions and their (plane boundary) images.

It is apparent that interaction with the plane boundaries has led to flagellar arrangements different from that in standard models. If we assume that the number, position, and rate of rotation of flagella are directly linked to the local strength of the rotating flows, then we may infer that the flagella are slightly skewed with oppositely polar arrangements. Moreover, as the flagella are $\gtrsim 6\ \mu$m long and

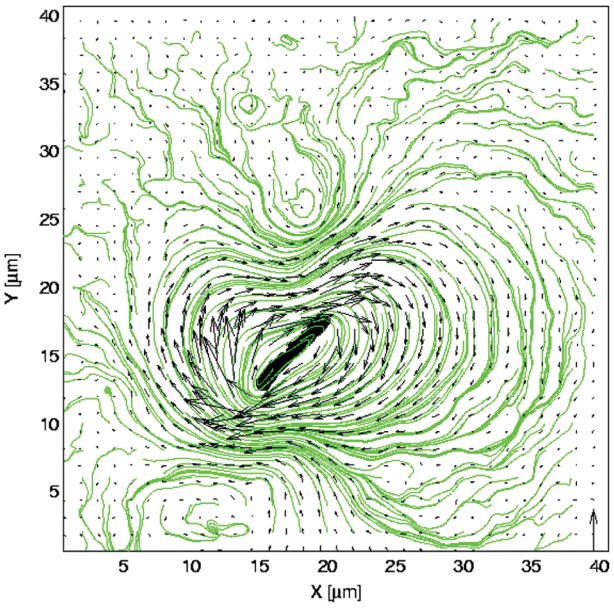

FIG. 1 (color). Stationary flow field (mean over 20 s) surrounding a stuck cell and corresponding streamlines (green) computed from a regular grid of initial points. The arrow in the lower right corner represents 10 $\mu\mathrm{m\,s}^{-1}$.

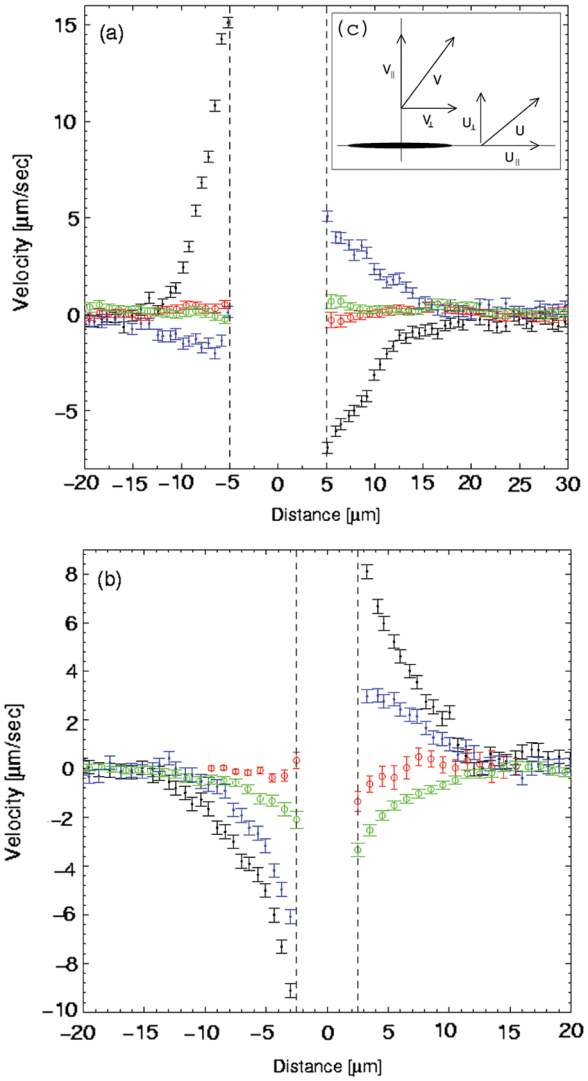

FIG. 2 (color). (a) perpendicular $U_\perp$ and parallel $U_\parallel$ components of velocity **U** as a function of the distance along the cell axis for a stuck cell (black & blue, respectively) and for a free swimming cell (red & green). (b) Same as for (a) except that data are for V and distance is transverse to the cell axis. (c) velocity components.

relatively stiff, it is then evident that the streamlines cross through the helical flagella. We hypothesize that this dynamic geometry can be understood in the following fashion: the clockwise (observed from the cell) rotating flagella interact strongly with the lower no-slip boundary and only weakly with the upper stress-free boundary. This leads to traction such that each flagellum rotates clockwise (viewed from above) about an axis at the body, countered by hydrodynamic interactions and mechanical properties of the flagella [11,12]. Such rotation, arrested by the body, can produce aggregation, or bundling, of flagella in two preferred oblique directions with respect to the bacterial body, as depicted in Fig. 3 (inset; simply illustrated by two flagella). We emphasize again that this geometry is quite different from the generally assumed backwardly oriented, propulsive arrangement of flagella. Here, there is no ''backward,'' since the cell is immobile. When flagella in these skewed, oppositely polar arrangements rotate about their axes, their helical shape ought to drive circulating flow of some form; rather than just propelling fluid parallel to the direction of each helical axis, the flow has a transverse component. To better understand this inference, in the next section, we investigate a computational model constructed according to the hypothesized geometry depicted in Fig. 3.

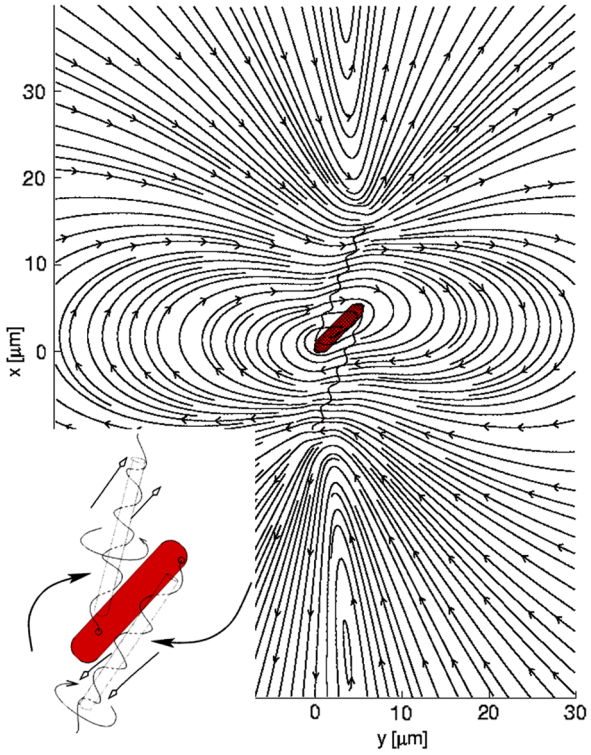

FIG. 3 (color online). Simulation streamlines in a plane (neglecting flows into the page) above an organism with two flagella close to an infinite wall. Inset: depiction of reduced model. Flagella are swept clockwise due to the asymmetry of the lower no-slip and upper (nominally) stress-free boundaries, and the resulting traction afforded the lower half of each flagellum.

(ii) Free swimming cells.—The magnitude of the flow generated by free swimming bacteria is much smaller and decays faster spatially than the flow due to stuck cells. Figure 2 shows the components of **U** and **V** for a cell swimming right to left, as a function of the distance from the cell. The flow speeds along the cell axis are an order of magnitude smaller than for a stuck bacterium. The error bars, due to Brownian motion of the marker beads, almost hide the flow (positive at the rear of the cell, negative at the front). The lateral flow $V_\perp$ is a little larger and negative everywhere due to the transverse thrust of the cell's curved trajectory.

(iii) Multicell PIV.—Figure 4 presents the flow field around several stuck cells in a thin layer of fluid. As well as the usual rotating flows about individuals, more complicated flows arise due to interactions between cells and their flagella. This leads to large scale rotating flows between cells and around the multicell complex, with immediate implications for biofilms. These flows are time dependent, presumably due in part to intermittences in the rotation of the many flagella involved in generating the flow. Such flows aid the transport of molecules for metabolism and interorganism communication, as well as of exuded polymers synthesis of biofilms [10].

Numerical simulations.—We shall show that asymmetric boundaries drive rotating flow, but one boundary is sufficient to reveal qualitative features, and is computationally less involved than two. Flow simulations were performed using the method of regularized Stokeslets [13–15], which provides expressions to compute fluid motion generated by forces that arise on the surface of a moving organism [14]. The velocity field due to the application of N surface forces is

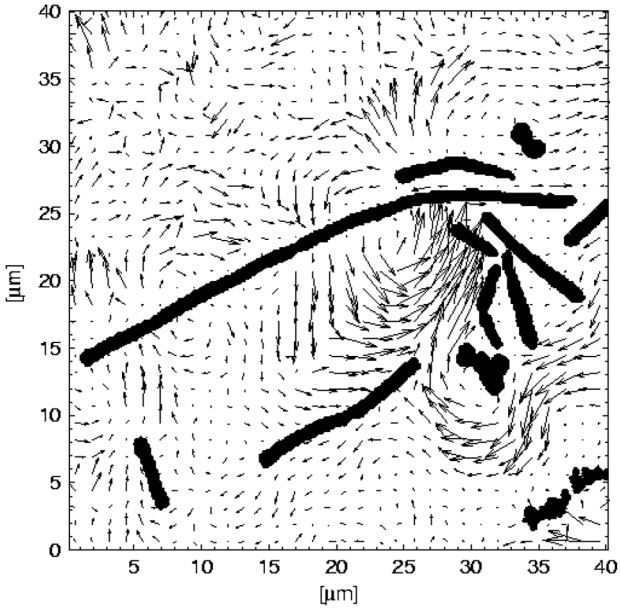

FIG. 4. Dynamic flowfield due to several stuck bacteria (both long and short) in a thin layer of fluid.

$$\mathbf{u}(\mathbf{x}) = \left(\frac{1}{8\pi\mu}\right)\sum_{k=1}^{N}\frac{(|\hat{\mathbf{x}}|^2 + 2\epsilon^2)\mathbf{f}_k + [\mathbf{f}_k \cdot \hat{\mathbf{x}}]\hat{\mathbf{x}}}{(|\hat{\mathbf{x}}|^2 + \epsilon^2)^{3/2}},$$

where $\hat{\mathbf{x}}$ is the vector from the force location $\mathbf{x}_k$ to the evaluation point $\mathbf{x}$. For a flow bounded by an infinite plane wall, the method is augmented with a system of images to automatically satisfy a no-slip condition [16].

Figure 3 shows the arrangement of the flagella and the streamlines of the computed flow. Despite the simplified model, there is a remarkable match with experimentally observed (Fig. 1) topologies of the fluid velocity, including the two off-axis eddies, supporting the hypothesized arrangement of flagella as inferred from experiments. The qualitative features of the Stokes flow solutions are independent of the flagellar angular velocity, ω_2: to agree with experiments, we find $\omega_2 = 7$ Hz. This rate of rotation of the flagella inferred from the computation together with the observed velocity of the marker beads strongly suggests that the rotation of lateral flagella bundles on stuck cells is hindered (effective rate ca. 10 times less than the ''standard'' 100 Hz). This result applies equally to [10], where similar bead velocities were found. The infinite plane wall is located at $z = 0$ μm with streamlines computed on $z = 2$ μm. The cell body is placed 0.022 μm from the wall, and has radius and length $R_b = 0.84$ μm and $L_b = 8$ μm, respectively. The fluid velocity is set to zero on the body surface. Both flagella have identical dimensions with length $L_h = 15.57$ μm, radius $R_h = 0.05$ μm, and pitch $P = 2.4$ μm. The angles between the flagella axes and the cell body axis are $\pi/8$, and both are left handed and rotate clockwise. Setting the flagella bundles to rotate with different rates induces a peanut shaped flow even more similar to Fig. 1. It is remarkable that the exponent of the decay with distance from the cell body on the numerical field is well fitted $k \sim 0.18$–0.25 μm^{-1}, in reasonable agreement with the experiments.

Summary and significance.—Interactions between bacteria and plane boundaries are complex: flagella do not align and bundle ''behind'' the cell body. Instead, they form a distributed envelope that drives a flow circulating around the body. That flow extends over dimensions greater than the cell body's; it decays exponentially in the near field with exponent approximately equal to $\frac{1}{4}$ μm^{-1}. This result contrasts starkly with the more localized flow in the vicinity of a translating bacterium. It is quite remarkable that these experimental results are well matched by computational modeling using the method of regularized Stokeslets, based on a simple, logically constructed geometric arrangement of the flagella. The consonance of experiment and computation yields substantial cross validation. We believe that it is possible to use our modeling technique to predict the geometry of flows surrounding *groups* of constrained cells (Fig. 4). Designing substrates that elicit appropriate arrangements of cell groups could lead to controllable, locally driven complex microflows.

What is the broader significance, for quorum sensing (i.e., cell-cell communication) and the development of biofilms? If cells signal each other, as in the quorum sensing step of biofilm initiation [17], they will do it while constrained, rather than freely swimming. Furthermore, ''real life'' situations of significance involve many interacting bacteria. Our observations, and those on glued cells [10], confirm that stuck bacterial groups with active flagella drive intermittent, complex, and far-ranging flows that appear to mix and provide advective transport.

The hydrodynamic interaction of microorganisms with each other and with surfaces is crucial in understanding the initiation of biofilms and the development of their polymer-mediated stability [2,18]. The present results, on extensive flows driven by immobile cells near a wall, are a crucial step in reaching that understanding.

Support: DOE W31-10t-ENG38 (L. H. C. & J. O. K.); NSF DMS 0612625 (R. O. & R. C.); EPSRC EP/D073308/1 (M. A. B.). We thank R. E. Goldstein, S. Ganguly and, especially, C. Dombrowski for useful comments.

*cisneros@physics.arizona.edu
+ricardo.ortiz@tulane.edu
‡m.bees@maths.gla.ac.uk

[1] L. H. Cisneros, R. Cortez, C. Dombrowsky, R. E. Goldstein, and J. O. Kessler, Exp. Fluids **43**, 737 (2007).
[2] R. Kolter and E. P. Greenberg, Nature (London) **441**, 300 (2006).
[3] M. Ito, N. Terahara, S. Fujinami, and T. A. Krulwich, J. Mol. Biol. **352**, 396 (2005).
[4] L. Turner, W. S. Ryu, and H. C. Berg, J. Bacteriol. **182**, 2793 (2000).
[5] R. M. Macnab, Proc. Natl. Acad. Sci. U.S.A. **74**, 221 (1977).
[6] C. Brennen and H. Winet, Annu. Rev. Fluid Mech. **9**, 339 (1977).
[7] H. C. Berg, *Random Walks in Biology* (Princeton University Press, Priceton, 1993).
[8] H. Aref, J. Fluid Mech. **143**, 1 (1984).
[9] S. R. Otto, A. N. Yannacopoulos, and J. R. Blake, J. Fluid Mech. **430**, 1 (2001).
[10] N. Darnton, L. Turner, K. Breuer, and H. C. Berg, Biophys. J. **86**, 1863 (2004).
[11] T. Goto, K. Nakata, K. Baba, M. Nishimura, and Y. Magariyama, Biophys. J. **89**, 3771 (2005).
[12] E. Lauga, W. R. Diluzio, G. M. Whitesides, and H. A. Stone, Biophys. J. **90**, 400 (2006).
[13] R. Cortez, SIAM J. Sci. Comput. **23**, 1204 (2001).
[14] R. Cortez, L. Fauci, and A. Medovikov, Phys. Fluids **17**, 031504 (2005).
[15] H. Flores, E. Lobaton, S. Méndez-Diez, S. Tlupova, and R. Cortez, Bull. Math. Biol. **67** 137 (2005).
[16] J. Ainley, S. Durkin, R. Embid, P. Boindala, and R. Cortez, J. Comput. Phys. **227**, 4600 (2008).
[17] M. R. Parsek and E. P. Greenberg, Trends Microbiol. **13**, 27 (2005).
[18] S. A. West, S. P. Diggle, A. Buckling, A. Gardner, and A. S. Griffin, Annu. Rev. Ecol. Evol. Syst. **38**, 53 (2007).